ChemComm

COMMUNICATION

View Article Online
View Journal | View Issue

Check for updates

Cite this: *Chem. Commun.*, 2023, **59**, 6897

Received 25th March 2023,
Accepted 10th May 2023

DOI: 10.1039/d3cc01464a

rsc.li/chemcomm

Open Access Article. Published on 16 May 2023. Downloaded on 2/2/2026 11:59:46 PM.
This article is licensed under a Creative Commons Attribution 3.0 Unported Licence.

Liquid-on-solid heterogeneous nucleation for a general synthesis of yolk–shell nanostructures†

Huiying Guo,[a] Huai Lin,[a] Zhouling Wu,[a] Ruoxu Wang *[b] and Hongyu Chen *[b]

Liquid-on-solid heterogeneous nucleation on solid nanoparticle seeds was achieved. Syrup solutions from a solute-induced phase separation (SIPS) process were heterogeneously nucleated on nanoparticle seeds to form syrup domains, similar to the "seeded growth" method in classical nanosynthesis. The selective inhibition of homogeneous nucleation was also confirmed and exploited for a high-purity synthesis, showing similarity between nanoscale droplets and particles. The seeded-growth of syrup could serve as a general and robust method to one-step fabricate yolk–shell nanostructures, with efficient loading of the dissolved substances.

At the nanoscale, the advance of synthetic capability paves the way towards sophisticated structures and functions.[1–3] Nanosynthesis often relies on the control over nucleation to fabricate nanoparticles (NPs, Fig. 1a), where heterogeneous nucleation (HEN) plays an important role in building appendant domains on existing nanoparticle seeds, achieving synergies among the multiple components.[4,5] A pre-condition for the HEN is the inhibition of homogeneous nucleation (HON), which creates additional nuclei that would compete for the growth materials. To date, HEN has only been utilized on solid materials,[6] and it would be meaningful to extend it to nanoscale liquid droplets, which have long been serving as reliable carriers and templates at the micron-scale.[7–9]

Recently, our group reported the bottom-up fabrication of liquid NPs through the HON *via* a solute-induced phase separation (SIPS).[10] More specifically, an aqueous solution of kosmotrope[11,12] would be excluded (nucleate) from a water-ethanol mixture, into uniform droplets of 10^{-21} to 10^{-18} L, which are then preserved by silica shells. Extending from this concept, the seeded growth of liquid domains *via* HEN would be highly desirable for creating hybrid nanostructures. However, unlike in solid nanosynthesis, the correlation between the product structure and the nucleation modes is easily concealed by the merging of liquid droplets (Fig. 1b).

In this work, we study the liquid-on-solid HEN by introducing solid NPs as seeds. Especially, we show that syrup—a sugar solution—could serve as a robust kosmotrope to initiate the HEN in a universal and controllable manner. Thus, the classical "seeded-growth" is achieved for a liquid, with a characteristic inhibition of the HON (Fig. 1a). Accordingly, a one-step synthesis of yolk–shell nanostructures was achieved with the syrup as the intermediate layer (Fig. 1c). The analogy between the solid and

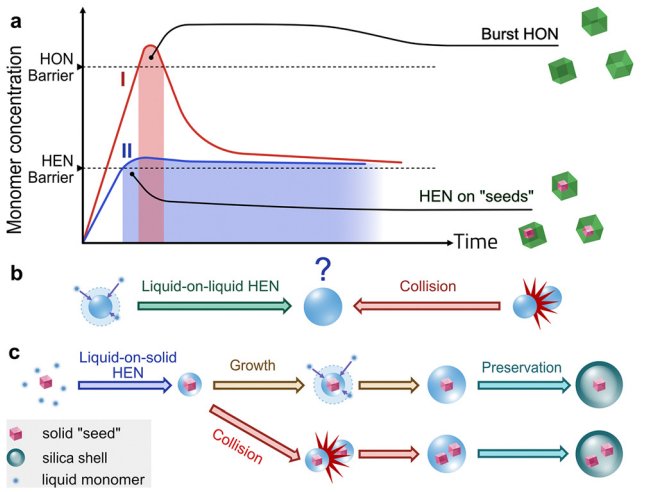

Fig. 1 (a) Schematic of LaMer model representing the correlation between the nucleation modes and specific types of products for solid NPs. Curve I and II I depict burst HON and HEN on "seeds", respectively. The shading of curve I and II indicate their nucleation stage, while the HON of curve II is inhibited by HEN, since the latter has a lower threshold. (b) Schematics representing the two possible pathways that are difficult to distinguish. (c) Schematics explaining how solid seeds could help distinguish the two pathways in a liquid-on-solid HEN.

[a] *Institute of Advanced Synthesis, School of Chemistry and Molecular Engineering, Nanjing Tech University, Nanjing 211816, China*
[b] *Department of Chemistry, School of Science, Westlake University, 310064, P. R. China. E-mail: chenhongyu@westlake.edu.cn, wangruoxu@westlake.edu.cn*

† Electronic supplementary information (ESI) available. See DOI: https://doi.org/10.1039/d3cc01464a

Open Access Article. Published on 16 May 2023. Downloaded on 2/2/2026 11:59:46 PM.
This article is licensed under a Creative Commons Attribution 3.0 Unported Licence.

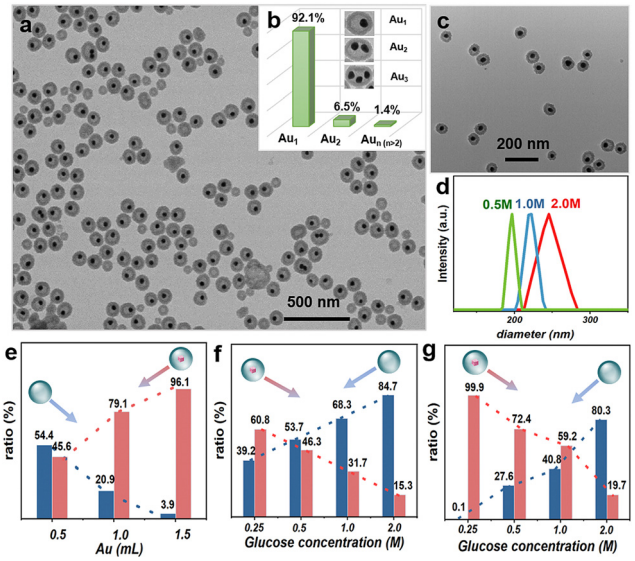

Fig. 2 (a) TEM image of the sample from the standard condition. (b) Histogram showing the ratio of yolk–shell nanostructures with different numbers of seeds among the Au_N@Syrup@Silica NPs. (c) TEM image of the product at 0.25 M glucose. (d) DLS chart of the samples with different concentrations of glucose. (e) Histogram showing that the percentage of the "empty" nanoshells (blue) decreases and that of Au@Syrup@Silica (red) increases with increasing concentration of AuNP seeds (after purification). (f) Histogram of the empty (blue) and Au@Syrup@Silica NPs (red) as glucose concentration decreases (before purification). (g) Histogram of the empty (blue) and Au@Syrup@Silica NPs (red) as glucose concentration decreases (after purification).

liquid nucleation processes is intriguing, opening immense possibilities for future synthetic designs of hybrid systems.

The standard condition uses glucose as the kosmotrope to initiate the SIPS process in a water-ethanol mixture, as modified from our previous report.[10] Specifically, citrate-stabilized AuNPs (d = 40 nm) were dispersed into an aqueous glucose solution, giving a translucent red liquid. It was added to a dilute ethanol solution of NaOH with 1 wt% of hydroxypropyl cellulose (HPC) under vortex mixing. The mixture gradually turned opaque, indicating that the glucose has successfully induced a phase separation to give liquid NPs. Then, tetraethyl orthosilicate (TEOS) was added to encapsulate and preserve the liquid NPs. After 6 h, the product was isolated by centrifugation, washed, and redispersed in ethanol.

In the transmission electron microscopy (TEM) images (Fig. 2a), the products show Au@Syrup@Silica yolk–shell nanostructures. Their size is around 80–120 nm, with a narrow size distribution (Fig. S1a, ESI†). With all AuNPs turned into the Au@Syrup@Silica NPs, no "naked" AuNP was observed. In our survey over 2000 NPs (Fig. S1c, ESI†), 30% of them are the "empty" silica nanoshells (Syrup@Silica). Among the Au@Syrup@Silica NPs, 92.1% of them contain only one AuNP (Au_1@syrup@Silica), whereas the rest contains multiple AuNPs in each shell (Au_N@Syrup@Silica, Fig. 2b).

As expected from the SIPS process, the yolk–shell nanostructure indicates a successful liquid-on-solid HEN, whereas the Syrup@Silica NPs likely arise from the HON (Fig. 1b). That is, the excluded glucose solution nucleates on the AuNPs and engulfs them, which process is supported by their narrow size distribution. The incomplete inhibition of HON may come from the insufficient concentration of seeds.

It should be noted that there are discernible gaps among the AuNPs in the Au_N@Syrup@Silica of Fig. 2b. There should have been no gap, if the AuNPs have collided prior to the HEN of syrup droplets. Hence, the phenomenon should be attributed to the collision and merging of the AuNP-containing liquid NPs (Fig. 1c).

To qualify for the liquid-on-solid HEN, it is critical to investigate the possibility that the AuNPs may be simply colliding and merging with the syrup NPs (Fig. 3a), though random and multiple collision would have led to wide size distributions. Previously, we have shown that adding TEOS at the beginning could capture very early stage intermediates.[13] However, we failed to capture the "naked" AuNPs and "empty" syrup droplets (the nanoshells) before their collision (Fig. 3b), indicating that collision is only a minor pathway.

The SIPS initiator (syrup) and AuNPs were added consecutively to decouple the two processes: The AuNP seeds dispersed in ethanol were added 10 s after the SIPS to give an opaque

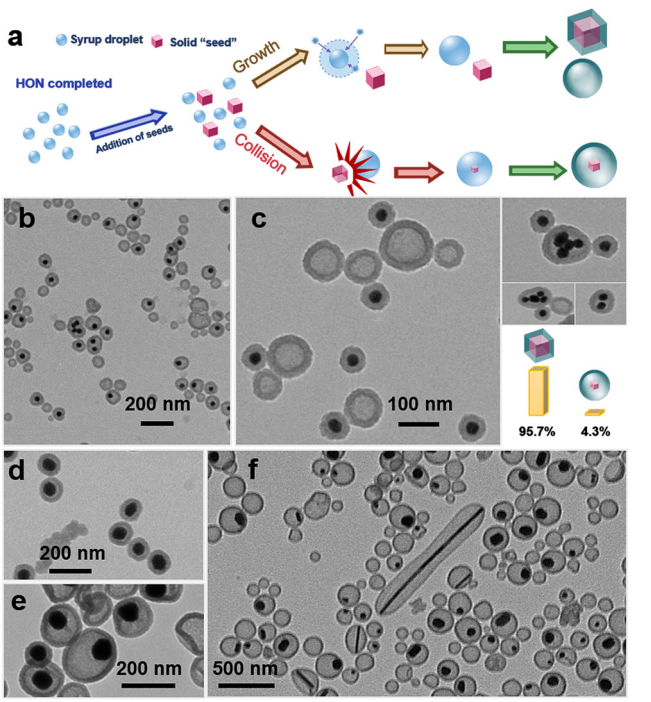

Fig. 3 (a) Schematics showing the decoupling of the phase separation and the addition of seeds. (b) TEM image of the trapped early-stage product. (c) TEM images of the product from the experiment in which phase separation and seed addition are decoupled. Inserted histogram shows 95.7% "naked" AuNP and 4.3% Au@Syrup@Silica. (d) and (e) TEM images showing the volume changes of the cavities induced by different concentrations of glucose: the pseudo core–shell structures with barely discernible cavities (d, 0.5 M glucose, 80 nm AuNPs); and the Au@Syrup@Silica NPs (e, 2 M glucose, 80 nm AuNPs). (f) Yolk shell structures made from the mixture of Ag nanostructures.

 This journal is © The Royal Society of Chemistry 2023

Open Access Article. Published on 16 May 2023. Downloaded on 2/2/2026 11:59:46 PM. This article is licensed under a Creative Commons Attribution 3.0 Unported Licence.

solution, then followed by the silica encapsulation. If collision is the dominant process, the product would be similar as the standard condition—the Au@Syrup@Silica NPs. Otherwise, HON of syrup would occur first, given the absence of seeds during the phase separation. The actual product coincides with the latter (Fig. 3c), where the vast majority are "empty" silica shells and "naked" AuNPs (95.7% among 1000 NPs surveyed), with only 4.3% being the Au@Syrup@Silica NPs (Fig. 3c). It confirms that the liquid-on-solid HEN is the dominant process.

The 4.3% of the AuNPs that turned into the Au@Syrup@Silica of Fig. 3c suggest that the collision pathway cannot be completely suppressed. In fact, the Au_N@Syrup@Silica with discernible gaps in Fig. 2b should also arise from the collision pathway. They are noticeably larger (100–150 nm, Fig. S1b, ESI†) than the Au_1@Syrup@Silica (80–120 nm). Moreover, 83% of the Au_N@Syrup@Silica have exactly 2 AuNPs, and their volume is also 2 times (Fig. S1d, ESI†), agreeing with the collision process. While collision is obviously occurring, it only accounts for a minor pathway (4.3–7.9%) in our experiments.

Most importantly, we found that the HON could be suppressed by increasing the seed concentration, which is characteristic for the seeded-growth of solid nanoparticles.[14–16] Since HEN has a lower threshold than HON (Fig. 1a), the presence of seeds would deplete the growth materials (syrup) in their vicinity and inhibit HON.[17] Thus, a higher seed concentration would occupy a higher percentage of the solution and effectively reduce the probability of HON. When the amount of seeds was tuned to 50%, 100%, and 150% of the standard condition, the proportion of empty nanoshells was 83.7%, 51.9%, and 34.2%, respectively (Fig. S2c, ESI†). Here, the samples were taken directly from the preparative solutions, to avoid the enrichment of heavier species during the purification. Further increase of the seeds led to increased Au_N@Syrup@Silica without gaps among the AuNPs (Fig. S2d, ESI†), indicating an extensive aggregation prior to the HEN of syrup.

To mitigate the collision pathway, the seed concentration was kept constant while the kosmotrope concentration was reduced: When the glucose concentration was reduced from 2 to 0.25 M, the empty nanoshells decreased from 84.7% to 39.2%. Notably, the cavities of the yolk–shell products became obviously smaller with a narrower size distribution (Fig. 2c and d), approaching a "pseudo-core–shell" structure with minimal gap. The empty nanoshells also decreased dramatically in size, such that they could be easily removed by centrifugation. Fig. 2f shows a clear trend that the percentage of empty nanoshells decreases with the lower glucose concentration, and the trend is more obvious after purification by centrifugation (Fig. 2e and g). The purified product is basically free of empty nanoshells (0.1%), highlighting the effective inhibition of HON. However, further decreasing of the glucose concentration may not be a practical way to promote the yield of yolk–shell products, due to the trend towards pseudo-core–shell structures.

These phenomena confirm that seeded-growth has been achieved and it is as applicable to the liquid droplets as it is to solid NPs. Seeded-growth has been widely practiced on solid materials, giving a series of sophisticated multi-component nanostructures.[15,16,18,19] The similarity between the two systems, particularly regarding nucleation and growth processes, means that the theories and designs could be borrowed for creating liquid-solid hybrid nanostructures.

To explore the generality of the liquid-on-solid seeded growth, 80 nm AuNPs were used as seeds. Pseudo-core–shell nanostructures were obtained (0.5 M glucose, Fig. 3d), which became yolk–shell nanostructures when more syrup is used (2 M glucose, Fig. 3e). To further explore the dependence on the shape of seeds, a mixture of Ag nanostructures from a one-pot citrate reduction was used, which is composed of nanorods, polyhedrons, and nanowires of different sizes. After the seeded-growth and silica encapsulation, all Ag seeds, regardless of the shape, gave yolk–shell nanostructures. As shown in Fig. 3f, the syrup domain obviously adopts a wetting conformation, encapsulating the entire surfaces of the citrate-stabilized seeds, as opposed to appendant domains on the side.

In practice, a variety of ligands could be used to stabilize and functionalize NPs. To test the ligand compatibility of the liquid-on-solid seeded-growth, the citrate-stabilized AuNPs were functioned by a series of thiol ligands with varying functional groups (Fig. 4j, orange zone). As shown in Fig. S4 (ESI†), there are no significant differences among the resulting Au@Syrup@Silica products, from ligands with multiple hydrophilic groups, to those with single hydrophilic groups, even to those with slight hydrophobicity (ligand **3**). Similar yolk–shell nanostructures were obtained when the ligands were respectively used for the mixture of Ag nanostructures of different shapes (Fig. S3 and S5, ESI†).

We used the nano-badges stabilized by cetyltrimethylammonium bromide (CTAB) and Ag nanowires stabilized by polyvinylpyrrolidone (PVP) as models to test the effects of common surfactants. However, the CTAB-stabilized seeds led to aggregation, whereas the PVP-stabilized seeds gave only core-shell NPs (Fig. S7, ESI†). For CTAB, this may be due to the strong hydrophobicity of its outward end. As to PVP, it is a chaotropic polymer, which could be incompatible with kosmotropic carbohydrates such as glucose. After a simple ligand exchange with the thiol-based ligands (**9**, **3**, **10**, Fig. 4j), yolk–shell products were obtained (Fig. 4g–i and Fig. S8, ESI†). It is remarkable that the complicated nanostructures to the extent of the Au nano-badges could still be well encapsulated by the syrup domains (Fig. 4d–f and Fig. S9, ESI†). Naturally, such method also works on AuNPs stabilized with CTAB or PVP (Fig. S10, ESI†). Besides, empty nanoshells also exist in the product. it is difficult to inhibit HON with larger seeds such as nano-badges and nanowires, since they cannot be dispersed as evenly as smaller nanoparticles are. Therefore, local HON could easily occur where there isn't a seed nearby, although empty nanoshells could be separated by centrifugation due to their significantly lower density.

Ligands with a large absorption cross-section for surface-enhanced Raman scattering (SERS) were also tested.[20] The Au@Syrup@Silica yolk–shell nanostructures obtained from the citrate-stabilized Au seeds show the characteristic peaks (Fig. 4k and Fig. S6, ESI†), indicating that the ligand exchange is successful and that the ligands are retained at the Au surface, *i.e.*, the seed-syrup interface.

Open Access Article. Published on 16 May 2023. Downloaded on 2/2/2026 11:59:46 PM.
This article is licensed under a Creative Commons Attribution 3.0 Unported Licence.

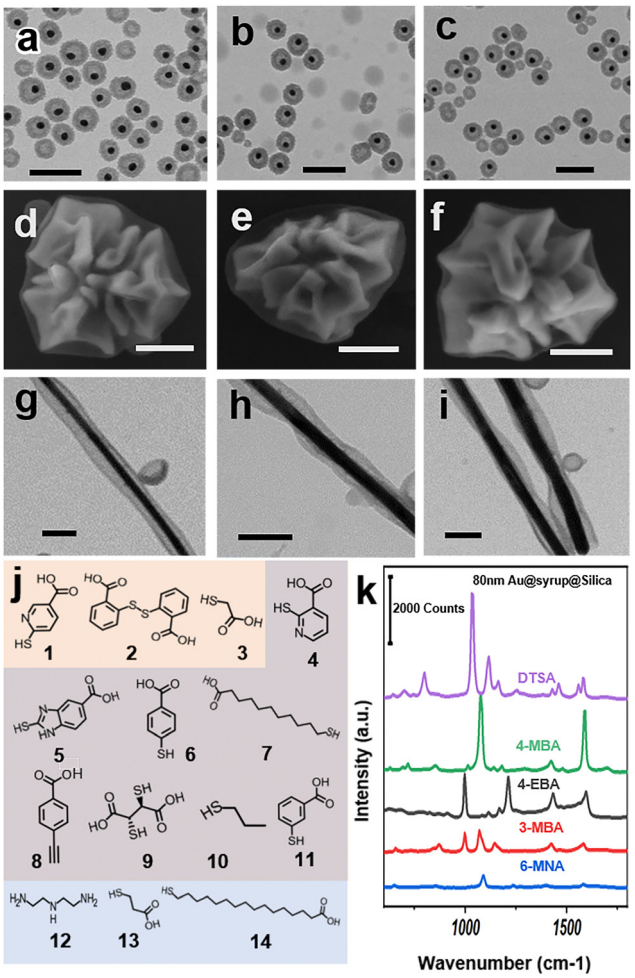

Fig. 4 (a)–(i) TEM images of yolk–shell nanostructures with different seeds and ligands: (a–c) Citrate-stabilized AuNP seeds after ligand exchange with **9**, **3** and **10**, respectively. (d–f) CTAB-stabilized Au nanobadges after ligand exchange with **9**, **3**, and **10**. (g–i) PVP-stabilized Ag nanowires after ligand exchange with **9**, **3**, and **10**. (j) A list of the compatible ligands. The orange-colored zone indicates ligands compatible with gold nanostructures, while the blue zone shows ligands compatible with silver nanostructures. (k) SERS spectra of the Au@Syrup@Silica NPs of which the seeds are exchanged with the SERS-active ligands. Scale bar: 200 nm.

In summary, we have shown that by introducing solid seeds, it is possible to manipulate the liquid-on-solid nucleation, similar to how HON and HEN are controlled in the traditional synthesis of solid nanoparticles. Based on this understanding, we have developed a general and robust method to fabricate yolk–shell nanostructures in one step. The results indicate that liquid-on-solid HEN is widely compatible with a large variety of ligands, in contrast to traditional ligand-controlled synthesis which is sensitive to ligand functional groups. This could be a result of the outstanding wettability of syrup droplet.[21] We expect that the method of liquid nucleation could be further exploited for advancing the synthetic controls at the nanoscale in the future.

We gratefully acknowledge the financial support from the National Natural Science Foundation of China: General Program (No. 21673117, HC), Major Program (No. 91956109, HC) and Zhejiang Provincial Natural Science Foundation of China: Major Program (No. 2022XHSJJ002, HC), Start-up Fund from Westlake University. We thank Westlake Center for Micro/Nano Fabrication for the facility support and technical assistance.

Conflicts of interest

There are no conflicts to declare.

Notes and references

1 F. Han, R. Wang, Y. Feng, S. Wang, L. Liu, X. Li, Y. Han and H. Chen, *Nat. Commun.*, 2019, **10**, 1548.
2 Z. Li, K. Xu, L. Qin, D. Zhao, N. Yang, D. Wang and Y. Yang, *Adv. Mater.*, 2022, e2203890, DOI: **10.1002/adma.202203890**.
3 Y. Ma, H. Zhang, R. Lin, Y. Ai, K. Lan, L. Duan, W. Chen, X. Duan, B. Ma, C. Wang, X. Li and D. Zhao, *Nat. Commun.*, 2022, **13**, 6136.
4 Y. Wang, J. He, C. Liu, W. H. Chong and H. Chen, *Angew. Chem., Int. Ed.*, 2015, **54**, 2022–2051.
5 Y. Xia, K. D. Gilroy, H. C. Peng and X. Xia, *Angew. Chem., Int. Ed.*, 2017, **56**, 60–95.
6 J. Zhou, M. Xu, Z. Jin, R. M. Borum, N. Avakyan, Y. Cheng, W. Yim, T. He, J. Zhou, Z. Wu, Y. Mantri and J. V. Jokerst, *Angew. Chem., Int. Ed.*, 2021, **60**, 26357–26362.
7 M. Błaszczyk, J. Sęk and Ł. Przybysz, *Microfluid. Nanofluid.*, 2022, **26**, 19.
8 M. Q. Giso, H. Zhao, P. T. Spicer and T. J. Atherton, *J. Colloid Interface Sci.*, 2022, **605**, 138–145.
9 Z. Luo and B. Liu, *Angew. Chem., Int. Ed.*, 2018, **57**, 4940–4945.
10 R. Wang, F. Han, B. Chen, L. Liu, S. Wang, H. Zhang, Y. Han and H. Chen, *Angew. Chem., Int. Ed.*, 2021, **60**, 3047–3054.
11 P. Luo, Y. Zhai, E. Senses, E. Mamontov, G. Xu, Y. Z and A. Faraone, *J. Phys. Chem. Lett.*, 2020, **11**, 8970–8975.
12 A. Casimiro, C. Weijers, D. Scheepers, Z. Borneman and K. Nijmeijer, *J. Membr. Sci.*, 2023, **672**, 121446.
13 R. Wang, Q. Wang, H. Guo and H. Chen, *Sci. China Mater.*, 2022, **65**, 1963–1970.
14 O. El-Zubir, E. L. Kynaston, J. Gwyther, A. Nazemi, O. E. C. Gould, G. R. Whittell, B. R. Horrocks, I. Manners and A. Houlton, *Chem. Sci.*, 2020, **11**, 6222–6228.
15 X. Zhao, V. D. Pawlik, D. Huo, S. Zhou, B. Yang and Y. Xia, *J. Phys. Chem. C*, 2021, **125**, 27394–27402.
16 L. Li, P. Zhang, W. Fu, M. Yang and Y. Wang, *Sens. Actuators, B*, 2018, **276**, 158–165.
17 Y. Feng, Y. Wang, X. Song, S. Xing and H. Chen, *Chem. Sci.*, 2017, **8**, 430–436.
18 G. Du, J. Pei, Z. Jiang, Q. Chen, Z. Cao, Q. Kuang, Z. Xie and L. Zheng, *Sci. Bull.*, 2018, **63**, 892–899.
19 Z. Lam, C. Liu, D. Su, H. B. Tao, H. Y. Wang, J. Chen, W. Xu, L. Zhang, Y. Zhu, L. Liu, Y. Han, H. Chen and B. Liu, *Nanoscale Adv.*, 2021, **3**, 177–181.
20 T. Xiang, J. Zong, W. Xu, Y. Feng and H. Chen, *Mater. Chem. Front.*, 2021, **5**, 465–471.
21 S. Lv, X. Zhang, X. Yang and Y. Zhai, *J. Phys.: Conf. Ser.*, 2022, **2152**, 012023.

 This journal is © The Royal Society of Chemistry 2023